

## Supporting Information

# Achieving High-Performance Thick-Film Perovskite Solar Cells with Electron Transporting Bingel Fullerene

Kangrong Yan<sup>a,†</sup>, Jiehuan Chen<sup>a,†</sup>, Huanxin Ju<sup>b</sup>, Feizhi Ding<sup>c</sup>, Hongzheng Chen<sup>a</sup>, Chang-Zhi Li<sup>a,\*</sup>

<sup>a</sup> MOE Key Laboratory of Macromolecular Synthesis and Functionalization, State Key Laboratory of Silicon Materials, Department of Polymer Science and Engineering, Zhejiang University, Hangzhou 310027, China

<sup>b</sup> National Synchrotron Radiation Laboratory, University of Science and Technology of China, Hefei, Anhui 230029, China.

<sup>c</sup> Division of Chemistry and Chemical Engineering, California Institute of Technology, Pasadena, CA 91125, USA

\* Corresponding author.

E-mail address: [czli@zju.edu.cn](mailto:czli@zju.edu.cn).

<sup>†</sup> Contributed equally to this work.

## 1. Experimental Procedures

### 1.1 General Information.

**Instrument.** <sup>1</sup>H NMR spectra were characterized by a Bruker Advance III 400 (400 MHz) nuclear magnetic resonance (NMR) spectroscope. MALDI-TOF MS spectra were measured on a Walters Maldi Q-TOF Premier mass spectrometry. UV-vis absorption spectra were recorded on a Shimadzu UV-2450 spectrophotometer. Cyclic voltammetry (CV) was done on a CHI600A electrochemical workstation with Pt disk, Pt plate, and standard calomel electrode (SCE) as working electrode, counter electrode, and reference electrode, respectively, in a 0.1 M Bu<sub>4</sub>NPF<sub>6</sub> CH<sub>2</sub>Cl<sub>2</sub> solution. The CV curves were recorded versus the potential of SCE, which was calibrated by the ferrocene-ferrocenium (Fc/Fc<sup>+</sup>) redox couple (5.1 eV below the vacuum level). Ultraviolet photoelectron spectrometer (UPS) measurements were conducted on an ESCALAB 250Xi (Thermo) system with a bias voltage of -9.8 eV. The SEM data were scanned by S-4800 (Hitachi) field-emission scanning electron microscope (FESEM). The PL spectra (both of steady state and transient spectra) are measured using FluoroMax-4 HORIBA Jobin Yvon spectrofluorometer. Field-effect transistors were measured by Keithley4200 SCS semiconductor parameter analyzer. Calculations were performed in the Density Functional Theory (DFT) framework as implemented in the GAUSSIAN software suite using the B3LYP exchange correlation functional and 6-31G(d) basis set.

**Materials.** All reagents and solvents, unless otherwise specified, were purchased from Aladdin, Aldrich, Energy Chemical, J&K Scientific Ltd and TANFENG. and were used without further purification.  $\text{CH}_3\text{NH}_3\text{I}$  (MAI) was purchased from Shanghai Materwin New Materials Co. Ltd.

## 1.2 Synthesis of Intermediates and fullerene ETMs<sup>1,2</sup>

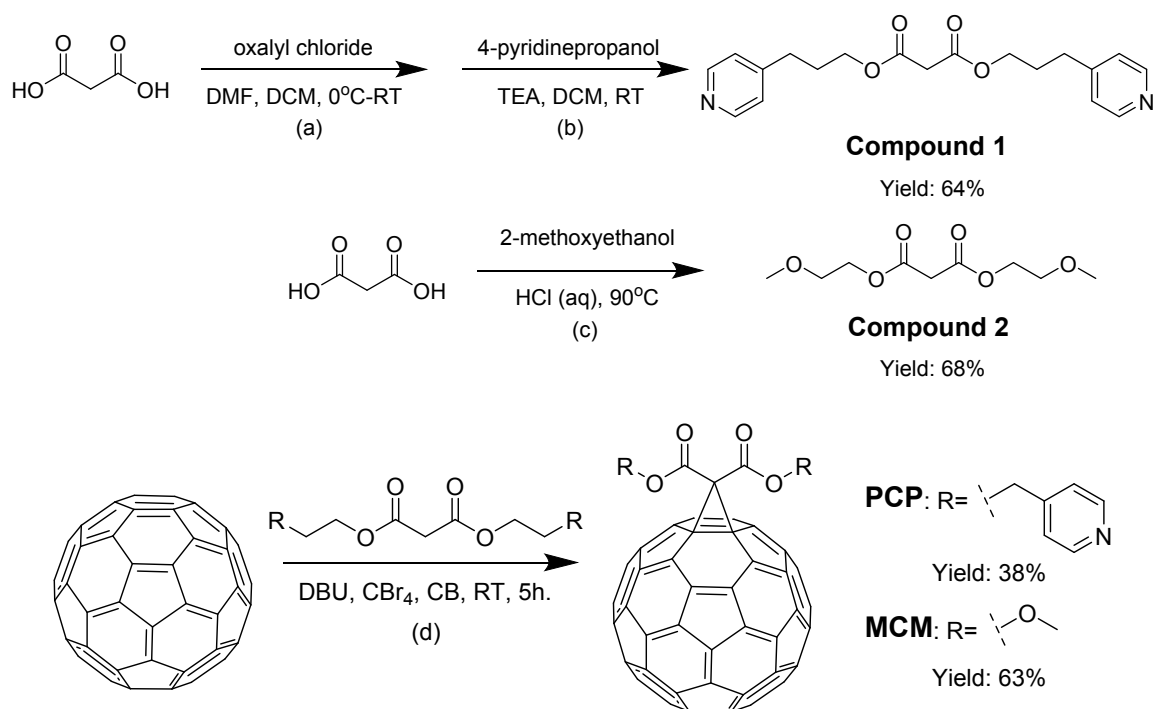


**Fig. S1.** Synthetic route. (a) oxalyl chloride, DMF, DCM, 0 °C-RT, 2h, 0 °C-RT, 2h. (b) 4-pyridinepropanol, DCM, TEA, RT, 10h, Ar, yield 64%. (c) 2-methoxyethanol, 36 wt% HCl solution, reflux at 90 °C, 5h, 68%. Synthetic route of fullerene ETMs. (d)  $\text{C}_{60}$ ,  $\text{CBr}_4$ , DBU, CB, RT, 3h, Ar, yield PCP 38%, MCM 63%.

**Bis(4-pyridinepropyl) malonate (Compound 1).** Malonic acid (380 mg, 3.65 mmol) was added into 250 ml round-bottom flask with 6 ml of dichloromethane (DCM), and then 4.02 ml 2 mol  $\text{L}^{-1}$  (8.04 mmol) oxalyl chloride in DCM was added. When mixed solution was cooled down in ice-water bath, 1 drop (0.2 ml) of *N,N*-dimethylformamide (DMF) added into flask. After drastic reaction, the mixture was up to room temperature (around 25 to 30 °C, RT) for 2 hours. Mixture was evaporated with rotatory evaporator and impure malonyl dichloride was obtained. Then 70 ml DCM was added into previous flask with impure malonyl dichloride, and another chemical 4-pyridinepropanol (1 g, 7.30 mmol) dissolved into 5 ml DCM was added into the flask, and 2 ml triethylamine TEA was gradually added. And the reaction was continuously proceeding for 10 hrs at room temperature. The mixture was poured into 100 ml of saturated potassium carbonate ( $\text{K}_2\text{CO}_3$ ) aqueous solution, and then it was extracted by DCM and water. Organic phase was dried over anhydrous sodium sulfate ( $\text{Na}_2\text{SO}_4$ ). After the solvent was removed, the crude product was purified by silica gel chromatographic column with the eluent ethyl acetate/methol (v:v=5:1). Faint yellow oil bis(4-pyridinepropyl) malonate (0.8 g, 64%) was obtained.  $^1\text{H}$  NMR (400 MHz,  $\text{CDCl}_3$ ,  $\delta$ ) 8.51 (d,  $J = 5.7$  Hz, 4H), 7.13 (t,  $J = 6.2$  Hz, 4H), 4.19 (t,  $J = 6.4$  Hz, 4H), 3.39 (s, 2H), 2.75 – 2.65 (m, 4H), 2.01 (dq,  $J = 9.1, 6.5$  Hz, 4H).

**Bis(2-methoxyethyl) malonate (Compound 2).** Malonic acid (2.9 g, 27.9 mmol) and 50 ml 2-methoxyethanol (Excessive, acted as reagent and solvent) was added into 100 ml round-bottom flask. Then 1 ml HCl solution (36 wt%) was added, and it was refluxed at 90 °C for 5 hrs. Mixture was evaporated with rotatory evaporator. And it was poured into 20 ml of saturated sodium bicarbonate (NaHCO<sub>3</sub>) aqueous solution, and then it was extracted by DCM and water. Organic phase was dried over anhydrous sodium sulfate (Na<sub>2</sub>SO<sub>4</sub>). After the solvent was removed, colorless oil bis(2-methoxyethyl) malonate (4.2 g, 68%) was obtained. <sup>1</sup>H NMR (500 MHz, CDCl<sub>3</sub>, δ) 4.31 (t, *J* = 9.5 Hz, 4H), 3.61 (t, *J* = 9.5 Hz, 4H), 3.47 (s, 2H), 3.39 (s, 6H).

**Di(3-(pyridin-4-yl)propyl) [60]fullerenyl malonate (PCP). Compound 1** (152.5 mg, 0.445 mmol), C<sub>60</sub> (317.7 mg, 0.441 mmol,) and tetrabromomethane (CBr<sub>4</sub>) (292.3 mg, 0.88 mmol) were dissolved into 70 ml of chlorobenzene (CB) in the 250 ml three-mouth flask. After bubbling argon gas for 30 min, 1,8-Diazabicyclo[5.4.0]undec-7-ene (DBU) (0.18 ml, ρ=1.018 g ml<sup>-1</sup>, 1.2 mmol) was added into the solution, and it stirred for 3 hrs at room temperature. The mixed solution was poured into silicagel column and then elution with toluene and C<sub>60</sub> was eluted at first. Then we eluted with DCM/methol (from 100:2 to 100:5, volume ratio) to afford khaki solid **PCP**, and purified again by chromatographic column to afford pure **PCP** (175.6 mg, 38%). <sup>1</sup>H NMR (400 MHz, CDCl<sub>3</sub>, δ) 8.53 (d, *J* = 5.6 Hz, 4H), 7.15 (d, *J* = 5.9 Hz, 4H), 4.60 – 4.49 (m, 4H), 2.87 – 2.78 (m, 4H), 2.20 (tt, *J* = 12.9, 6.4 Hz, 4H). C<sub>79</sub>H<sub>20</sub>O<sub>4</sub>N<sub>2</sub>, Exact Mass = 1060.14, MS (MALDI-TOF) = 1061.271.

**Di(1-methoxyethyl) [60]fullerenyl malonate (MCM). Compound 2** (260 mg, 1.18 mmol), C<sub>60</sub> (1.021 g, 1.42 mmol) and CBr<sub>4</sub> (785 mg, 5.16 mmol) dissolved into 50 ml of dichlobenzene (DCB) in the 250 ml three-mouth flask. After bubbling argon gas for 30 min, DBU (0.44 ml, 29.3 mmol) was gradually added into the solution, and it stirred for 3 hrs at room temperature. The mixed solution was poured into silicagel column and then elution with toluene and C<sub>60</sub> was eluted at first. Then we eluted with DCM/methol (from 100:2 to 100:5, volume ratio) to afford brown solid **MCM**, and purified again by chromatographic column to afford pure **MCM** (700 mg, 63%). <sup>1</sup>H NMR (400 MHz, CDCl<sub>3</sub>, δ) 4.65 (t, *J* = 9.4 Hz, 4H), 3.78 (t, *J* = 9.4 Hz, 4H), 3.44 (s, 6H). C<sub>69</sub>H<sub>14</sub>O<sub>6</sub>, Exact Mass = 938.08, MS (MALDI-TOF) = 937.897.

### 1.3 Computational details for modeling binding energies

Density functional theory is used for evaluating the binding energies between the two ETMs with the Pb<sup>2+</sup> cation. For the sake of computational efficiency, the interaction between the Pb<sup>2+</sup> cation and the two ETMs is modeled by the interaction of the Pb<sup>2+</sup> cation with the *p*-methyl pyridine and dimethyl ether. The binding energies are calculated using the B3LYP hybrid density functional. Two sets of basis functions are used for calibration purposes: the smaller 6-31G\*/LanL2DZ basis set (with LanL2DZ effective core potential basis on Pb and 6-31G\* all-electron basis on the rest elements) and the larger Def2-TZVP all-electron basis for all elements. The calculated binding energies are summarized in **Table S2 & S3**. All geometries are obtained from geometry optimization at the B3LYP/6-31G\*/LanL2DZ level of theory. All calculations are performed using the Gaussian 09 quantum chemistry package.

#### 1.4 Optoelectronic characterization

**PVSC fabrication:** The ITO coated substrates were cleaned sequentially in detergent (2%vol Hellmenex), deionized water, acetone, and isopropanol ultrasonic bath for 15 min, respectively. After then, the substrates were dried in nitrogen flow and cleaned by UV-Ozone treatment for 20 min before using. NiO<sub>x</sub> substrate was prepared by spin coating precursor solution (Nickel(II) nitrate hexahydrate: Ethylenediamine = 1M: 1M in ethylene glycol ) on ITO glass and annealed at 300 °C for 1h, detail information could be found in other report.<sup>3</sup> MAI and PbI<sub>2</sub> were mixed by 1:1 molar ratio in DMAc and NMP (4:1) mixture with the concentration of 1.4 M. Before spin-coating the perovskite layer, the precursor solution and NiO<sub>x</sub> substrate were heated at 70 °C. The spin-coating process was 1000 rpm for 10 s, and 4000 rpm for 30 s, and started initially after dropping the heated precursor to the heated substrate, after that 50 µl toluene was dropped at around 15 s during the second procedure, followed by annealing at 100 °C for 2 min. PCP or MCM solution (10 mg/ml in CB) was spin-coated on perovskite at 2000 rpm for 30 s; BCP (0.5 mg/ml in Ethanol) was spin-coated at 3000 rpm for 30 s, followed by deposited 100 nm Ag in vacuum chamber under high vacuum of 5x10<sup>-4</sup> Pa. The device area is 0.115 cm<sup>2</sup>, which is defined by the cross section of Ag and ITO.

**PVSC characterization:** The current density-voltage (*J-V*) characteristic curves were recorded on the Keithley source unit under AM 1.5G 1 sun intensity illumination (100 mW cm<sup>-2</sup>) by a solar simulation from Enli Technology, and the light intensity was calibrated with a standard photovoltaic reference cell. The EQE spectrum was measured using a QE-R Model of Enli Technology.

**FET Device Fabrication and Characterization:** Highly doped silicon substrates (1 cm<sup>2</sup>) with 300 nm SiO<sub>2</sub> were used for field-effect transistor fabrication. The substrates were modified with divinyltetramethyldisiloxanebis(benzocyclobutene) (BCB) (Dow Chemicals, USA) thin-layers, which was spin-coated from a mesitylene (Fluka) solution ( $V_{\text{BCB}}:V_{\text{mesitylene}}=1:30$ ) and thermally cross-linked on a hotplate in a N<sub>2</sub> glovebox. Then, fullerene (**PCP** or **MCM**) solution (10 mg ml<sup>-1</sup> in chloroform) was spin-coated onto the substrates, followed by baking at 70 °C for 2 h in N<sub>2</sub>. FETs were fabricated by depositing source and drain electrodes (50 nm Ag), using a shadow mask with channel length (L) of 50 µm and width (W) of 1 mm in a top-contact, bottom-gate configuration. The performance of the FETs was measured under dark by Keithley4200 SCS semiconductor parameter analyzer in a glove box. The mobility was calculated from saturation regime and presented as mean ± SD.

**UPS measurements:** The perovskite layers were fabricated by the method in Experimental Section and the **PCP** (or **MCM**) solution (1.0 mg ml<sup>-1</sup> in chlorobenzene) were spin-coated on the top of perovskite layer at a rate of 4,000 rpm to form the ultrathin fullerene layer. Ultraviolet photoemission spectrometer (UPS) measurements were conducted on an ESCALAB 250Xi (Thermo) system with a bias voltage of -9.8 eV in the ultra-high vacuum system. He I (21.22 eV) excitation lines from a helium plasma discharge lamp were employed for the UPS measurements. The instrumental resolution was 0.05 eV for UPS.

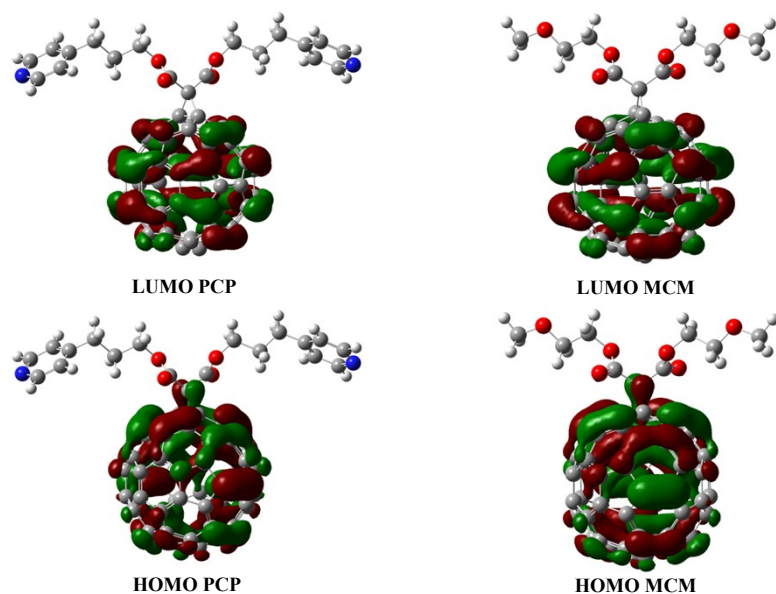


**Fig. S2.** Calculated frontier molecular orbitals of PCP and MCM.

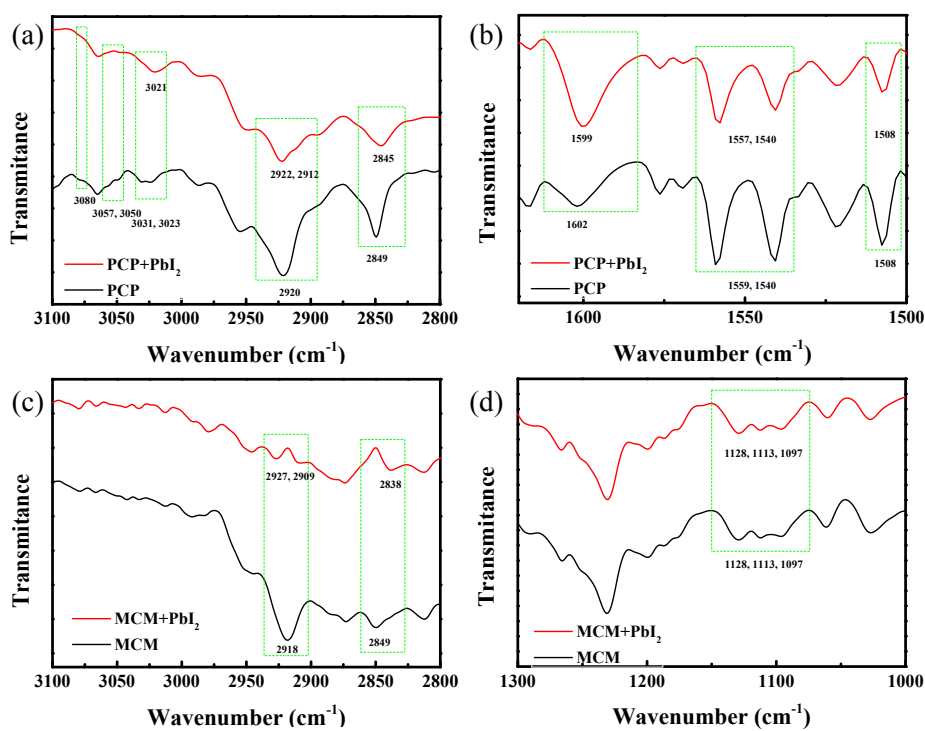


**Fig. S3.** The FTIR spectra of pure fullerenes and fullerenes:  $\text{PbI}_2$  mixtures. (a) and (b) represent the C-H stretching vibration and the C=C and C=N stretching vibration of pyridine aromatic backbone of PCP and PCP:  $\text{PbI}_2$ , respectively. (c) and (d) represent the C-H stretching vibration and the C-O stretching vibration of MCM and MCM:  $\text{PbI}_2$ , respectively.

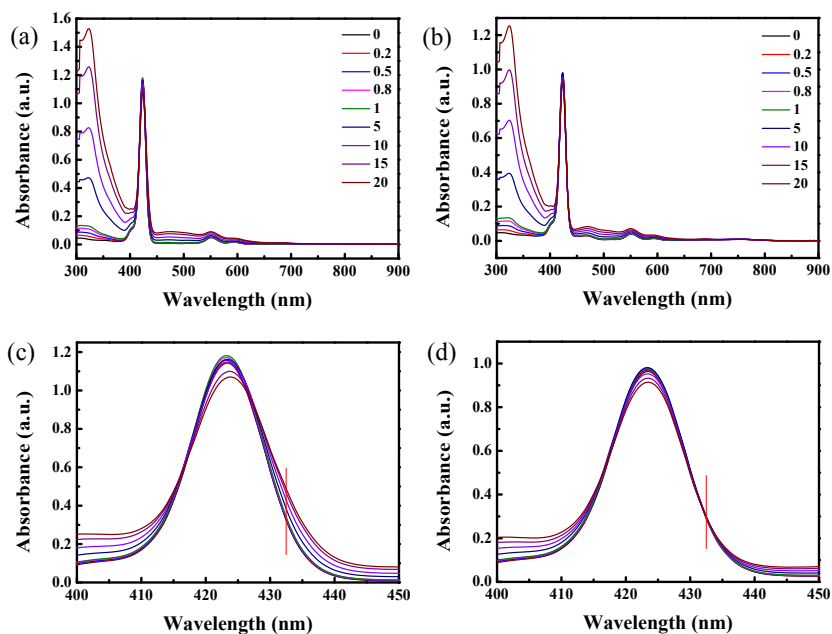


**Fig. S4.** UV-vis titration files of fullerenes and Zinc porphyrins (Zn-TBP). (a) and (b) represent the UV-vis spectra PCP and MCM titrating Zn-TBP, respectively. (c) and (d) the detail of enlarged UV-vis spectra from 400 to 450 nm. The concentration of Zn-TBP in  $\text{CH}_3\text{Cl}$  is  $2 \times 10^{-6}$  mol  $\text{L}^{-1}$  with the varied fullerene from 0 to 20 equivalent.

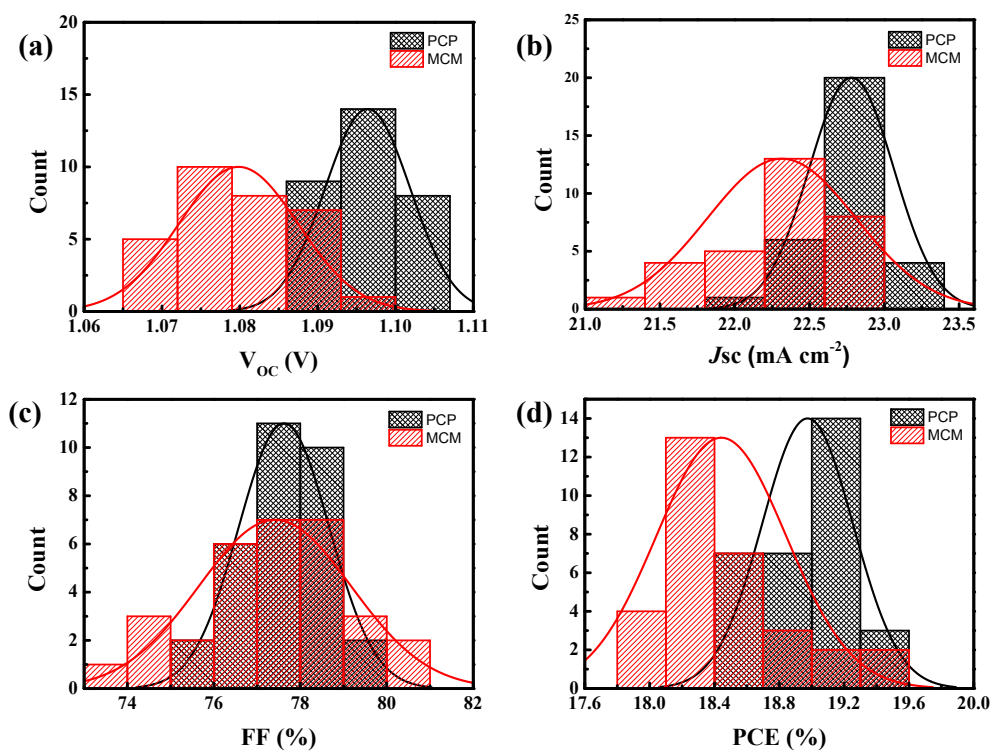


**Fig. S5.** The histogram of device performance based on 30 devices.

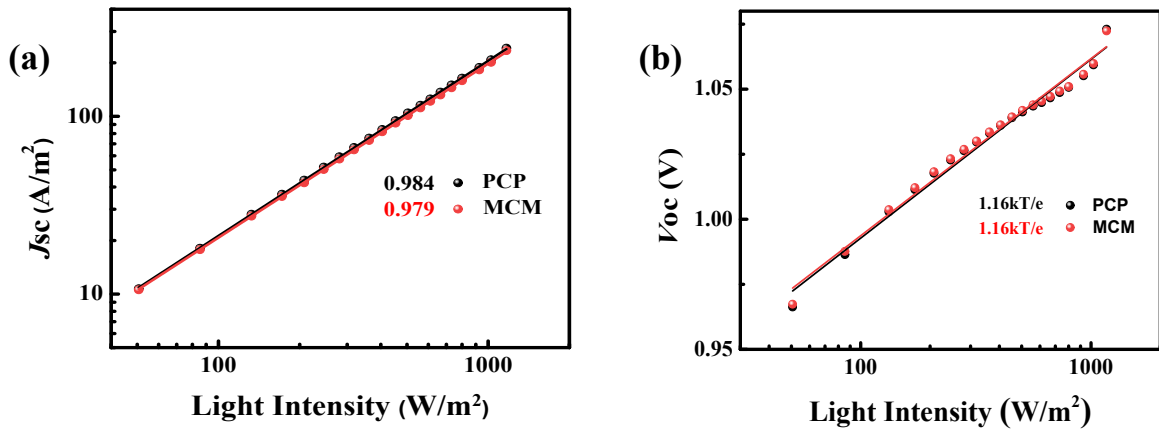


**Fig. S6.** (a) Measured  $J_{SC}$  of cells with different ETMs plotted against light intensity (symbols) on a logarithmic scale. Fitting a power law (solid lines) to these data yields  $\alpha$ . (b) Measured  $V_{OC}$  of cells with different ETMs plotted against light intensity (symbols), together with linear fits to the data (solid lines).

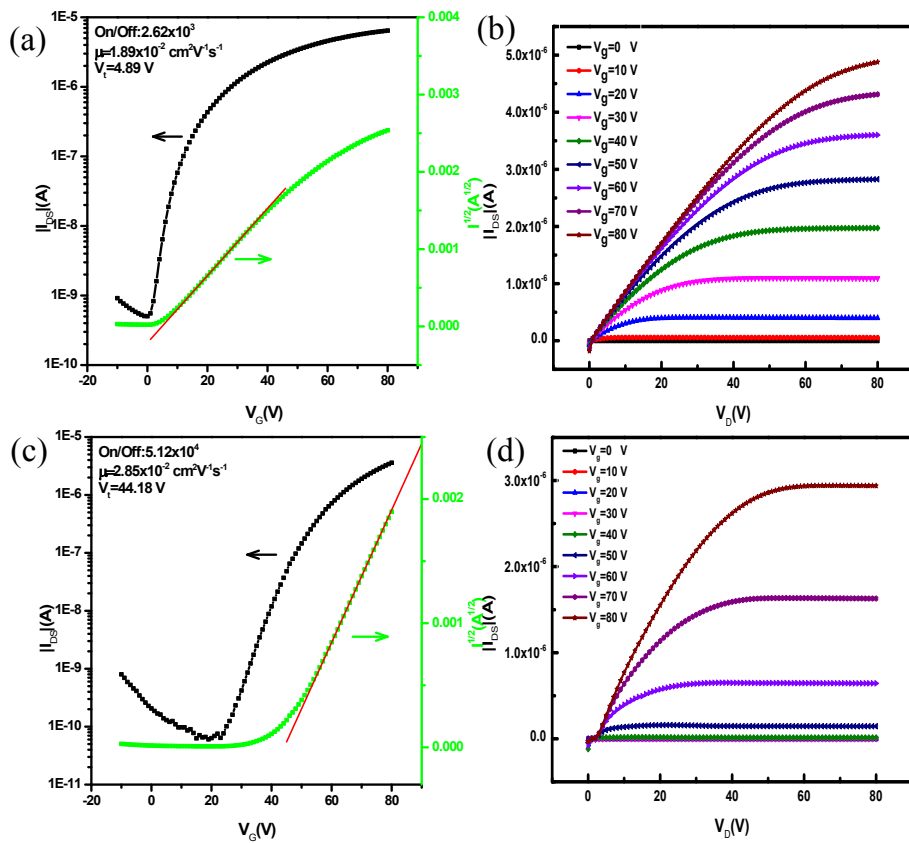


**Fig. S7.** (a) and (b) are transfer and output characteristics for PCP; (c) and (d) are transfer and output characteristics for MCM. FET devices adapt top-contact and bottom-gate geometry with divinyltetramethyldisiloxane-bis(benzocyclobutene) (BCB) buffer layer atop of silicon substrate and silver electrode. Fullerene sample films were subjected 70 °C annealing before electrode deposition.

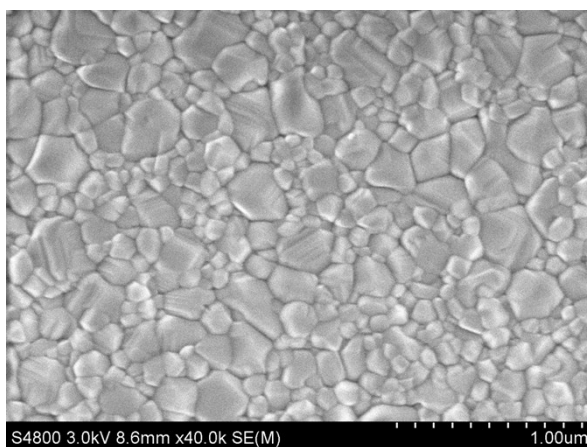


**Fig. S8.** A top-view SEM image of the perovskite film from the glass/ITO/ $\text{NiO}_x$ /MAPbI<sub>3</sub> sample.

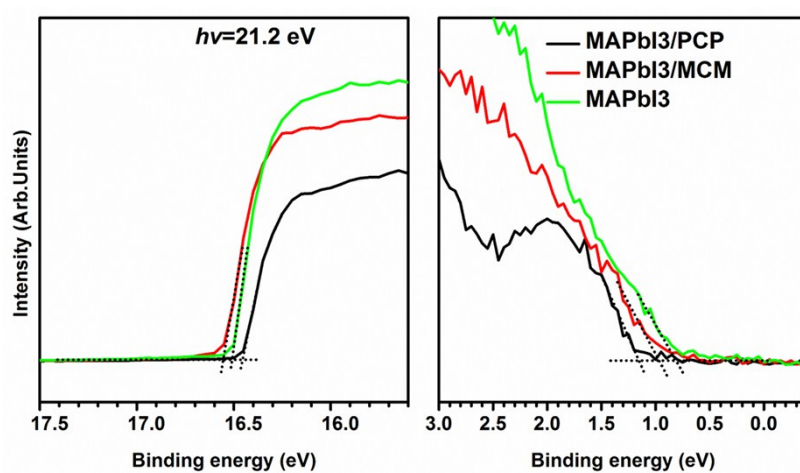


**Fig. S9.** UPS spectra of the perovskite surface with and without incremental coverage of fullerene layers, UPS He I spectra yield the valence band region of the plain surfaces,  $\text{VBM} = -h\nu - E_{\text{Femi}} + E_{\text{Cutoff}}$ ,  $h\nu = 21.2$  eV. UPS samples are perovskite/PCP (black line), perovskite/MCM (red line) and perovskite (green line). The perovskite layers were fabricated seen Experimental Section, and  $1 \text{ mg ml}^{-1}$  fullerenes (PCP or MCM) were spin-coated on the perovskite at 2,000 rpm.

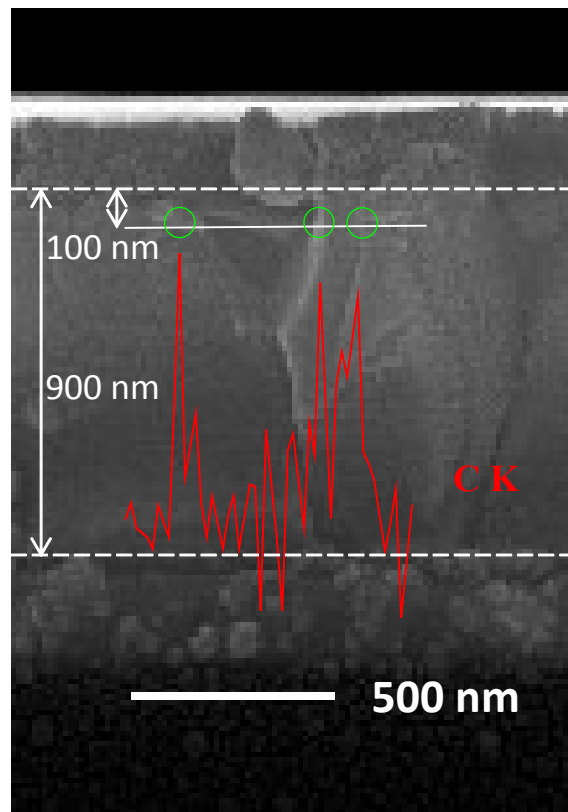


**Fig. S10.** The cross-section SEM image and EDX profile of perovskite film covered with fullerene; the EDX results show the sharp increase of carbon signals is representative for the fullerene rich at the perovskite GB regions. The white line is representative for the track of EDX scanning; the red curve is the carbon signal intensity profile; and the green cycles are fullerene rich zones at the perovskite GB regions.

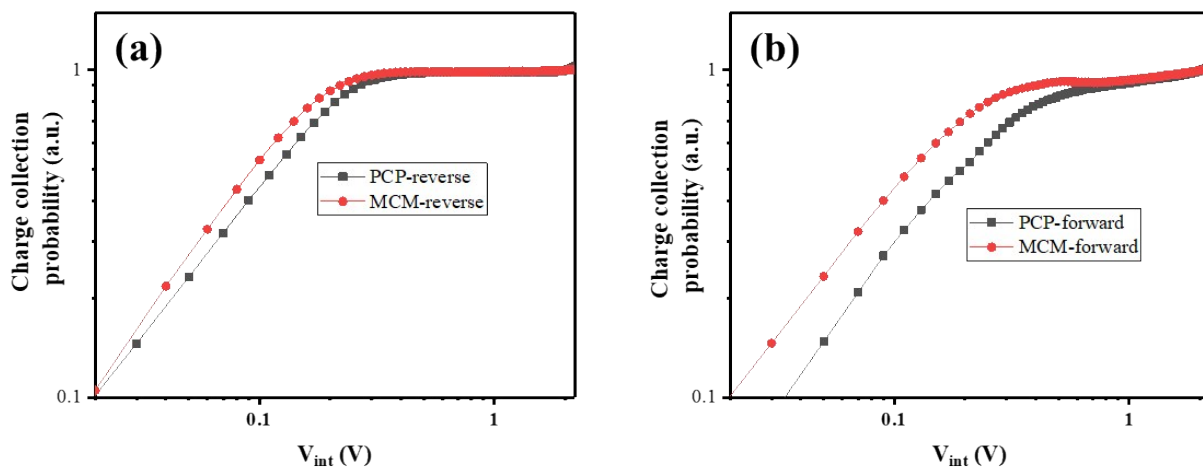


**Fig. S11.** Charge collection probability as a function of internal voltage for cells with different ETMs and different scanning directions.

**Table S1.** The data of calculated frontier molecular orbitals of PCP and MCM.

ETM	PCP (eV)	MCM (eV)
LUMO+1	-3.11	-3.11
LUMO	-3.16	-3.17
HOMO	-5.74	-5.75
HOMO-1	-5.87	-5.88

**Table S2.** Summarized binding energy between Pb<sup>2+</sup> and the *p*-methyl pyridine N-atom.

	Smaller basis	Bigger Basis
	6-31G*//LanL2DZ	Def2-TZVP
Pb <sup>2+</sup>	-2.65	-192.14
MePy	-287.60	-287.71
MePy-Pb <sup>2+</sup>	-290.45	-480.03
Binding energy (kcal mol <sup>-1</sup> )	-120.51	-113.57

**Table S3.** Summarized binding energy between Pb<sup>2+</sup> and the dimethyl ether O-atom.

	Smaller basis	Bigger Basis
	6-31G*//LanL2DZ	Def2-TZVP
Pb <sup>2+</sup>	-2.65	-192.14
Me <sub>2</sub> O	-155.02	-155.09
Me <sub>2</sub> O-Pb <sup>2+</sup>	-157.82	-347.36
Binding energy (kcal mol <sup>-1</sup> )	-89.40	-78.89

## References

1. C. Bingel, *Chem. Ber.*, 1993, **126**, 1957-1959.
2. T. Wei, M. E. Perez-Ojeda and A. Hirsch, *Chem. Commun.*, 2017, **53**, 7886-7889.
3. J. You, L. Meng, T.-B. Song, T.-F. Guo, Y. (Michael) Yang, W.-H. Chang, Z. Hong, H. Chen, H. Zhou, Q. Chen, Y. Liu, N. D. Marco and Y. Yang, *Nat. Nanotech.*, 2015, **11**, 75-81.